Clays and Clay Minerals, Vol. 33, No. 1, 1–14, 1985.

DEHYDROXYLATION, REHYDROXYLATION, AND STABILITY OF KAOLINITE

VERNON J. HURST
Geology Department, University of Georgia
Athens, Georgia 30602

ALBERT C. KUNKLE
Research Department, J. M. Huber Corporation
Macon, Georgia 31298

Abstract—From hydrothermal experiments three pressure-temperature-time curves have been refined for the system Al_2O_3-SiO_2-H_2O and reversal temperatures established for two of the principal reactions involving kaolinite. The temperatures of three isobaric invariant points enable the Gibbs free energy of formation of diaspore and pyrophyllite to be refined and the stability field of kaolinite to be calculated. The maximal temperature of stable kaolinite decreases from 296°C at 2 kb water pressure to 284°C at water's liquid/vapor pressure, and decreases rapidly at lower pressures. On an isobaric plot of $[H_4SiO_4]$ vs. $°K^{-1}$, kaolinite has a wedge-shaped stability field which broadens toward lower temperature to include much of the $[H_4SiO_4]$ range of near-surface environments. If $[H_4SiO_4]$ is above kaolinite's stability field and the temperature is <100°C, halloysite forms rather than pyrophyllite, an uncommon pedogenic mineral. Pyrophyllite forms readily instead of kaolinite above 150°C if $[H_4SiO_4]$ is controlled by cristobalite or noncrystalline silica.

Kaolinite and a common precursor, halloysite, are characteristic products of weathering and hydrothermal alteration. In sediments, relatively little halloysite has survived due to its low dehydration temperature and instability at low water pressure, but kaolinite commonly has survived since the Devonian Period. In buried sediments, the water pressure and $[H_4SiO_4]$ requisite for stable kaolinite generally are maintained. In oxidized sediments and in pyritic reduced sediments, kaolinite commonly has survived, but where alkalies, alkaline earths, or aqueous iron has concentrated in the pore fluid, kaolinite has tended to transform to illite, zeolites, berthierine, or other minerals.

Key Words—Dehydroxylation, Gibbs free energy, Halloysite, Hydralsite, Hydrothermal, Kaolinite, Pyrophyllite.

INTRODUCTION

The dehydroxylation of kaolinite at atmospheric pressure has been described extensively in scores of papers and patents during the last 60 years. Although several early papers (Van Nieuwenberg and Pieters, 1929; Schachtschabel, 1930; Hill, 1953; Saalfeld, 1955; von Dietzel and Dhekne, 1957) demonstrated rehydroxylation, the rehydroxylation process has not been studied in detail. Roy and Brindley (1956) hydrothermally treated 'meta' phases of kaolinite, dickite, and halloysite and found that all rehydroxylated to kaolinite. Their finding that rehydroxylation takes place at 370°C and 20,000 psi and their conclusion that pressure affects rehydroxylation less than temperature are incompatible with recent work.

Although early experimental work on the system Al_2O_3-SiO_2-H_2O (Roy and Osborn, 1954; Carr and Fyfe, 1960; Aramaki and Roy, 1963; Velde and Kornprobst, 1969) gave different boundaries for the stability field of kaolinite and different dehydroxylation products, they did sharpen awareness of the distinction that must be made between stability and synthesis fields and of the need to consider additional variables.

Garrels and Christ (1965) calculated the stability of kaolinite at 25°C and 1 bar, with the activities of H_4SiO_4, Al^{3+}, and AlO_2^- as variables. A subsequent investigation of the synthesis field of kaolinite by Eberl and Hower (1975) varied the Si/Al ratio of hydrothermal charges without explicitly treating activities of dissolved species. In 1977, Walther and Helgeson presented a diagram of stability relations for the system Al_2O_3-SiO_2-H_2O at 1 kb, with temperature and the activity of H_4SiO_4 as variables. Hemley *et al.* (1980) published stability relationships for this system at 1 kb, 2 kb, and pressures along the liquid-vapor curve of water. Their diagrams were calculated from thermodynamic data derived from their measurements of aqueous silica at 1 kb invariant points.

To refine the Gibbs free energies needed to calculate the stability field of kaolinite, more than 250 hydrothermal runs have been made with kaolinite and metakaolinite. These runs yielded three pressure-temperature-time curves and two important reaction reversals which, following Hemley *et al.* (1980), yielded three isobaric invariant points in the system Al_2O_3-SiO_2-H_2O.

EXPERIMENTAL PROCEDURE AND MATERIALS

The hydrothermal runs were made in cold-seal rod pressure vessels. Charges of 0.0828 g clay and 0.0828 g H_2O, were sealed in metal tubes, Ag or Pt when the charge pH was ~7, Au when the pH was lower. The tubes were weighed before and after runs to check for leaks. The charges were quenched by plunging the pressure vessel into cold water. The accuracy of experimental temperatures and pressures is estimated to be ±2°C and ±3%, respectively.

Metakaolinite for the first 100 runs was a commercial calcination product sold by the J. M. Huber Corporation, their designation 80-C. It was 85% finer than 2 μm and yielded no X-ray diffraction pattern. Metakaolinite for subsequent runs was Rio Capim kaolin (Hurst and Basio, 1975), degritted without dispersant and fired for 2 hr at 650°C. Runs with metakaolinites prepared from a variety of kaolins from Georgia, England, and Brazil showed that transformation temperatures were hardly affected by source when run duration was >3 days. The natural kaolinite that was used was degritted Rio Capim kaolin. The silicic acid was Baker analyzed reagent containing 10.6% water.

Phase identifications were based on X-ray powder diffraction (XRD) patterns obtained with a Norelco diffractometer (CuKα radiation), on crystal morphology, or on electron diffraction patterns obtained with a Siemens 101 or Philips 400 electron microscope. Recorded peak intensities are the average of four XRD measurements made on different portions of two mounts.

REACTION KINETICS

Experimental work in the system Al_2O_3-SiO_2-H_2O generally has been impaired by sluggish reaction rates, metastable phases, and difficulty in establishing equilibrium by reaction reversal. These problems can be largely overcome by using charge materials of high entropy and by lowering the pH. The reaction Kaolinite +2 Quartz = Pyrophyllite + H_2O, for example, can be accelerated by these means enough for reversal within 12 days over a temperature interval smaller than 5°C at 260°C.

Each mineralogical transformation involving kaolinite takes place through dissolution and recrystallization, and can be regarded as the sum of two reactions. Reaction (1) below, for example, can be described as the sum of reaction (a), breakdown of a mineral to form ions, and reaction (b), recombination of ions to form another mineral:

(a) $\text{Pyrophyllite} + 10H_2O = 2Al^{3+} + 4H_4SiO_4 + 6OH^-$

(b) $2Al^{3+} + 2H_4SiO_4 + 6OH^- = \text{Kaolinite} + 5H_2O$

---

(1) $\text{Pyrophyllite} + 5H_2O = \text{Kaolinite} + 2H_4SiO_4.$

As shown by the equations, the direction of the phase change is independent of pAl^{3+} and pH, but strongly dependent upon pH_4SiO_4. Reaction rate depends upon all three. Below pH 8, the activity of H_4SiO_4 is essentially independent of pH, which can be lowered to increase the activity of aqueous aluminum and thus accelerate reaction, without changing the position of the phase boundary. The lowering of pH to accelerate reaction becomes less effective above 300°C, where dissociation of HCl decreases rapidly (Hemley, 1959; Henley, 1973).

RESULTS

Two sets of data were obtained, one from hydrothermal runs, the other from thermal dehydroxylations at atmospheric pressure.

Hydrothermal runs

When a metakaolinite-water slurry was heated <200°C, rehydroxylation was very slow, a reaction time of a week or more was required for rehydroxylation to be detectable by X-rays. Above 200°C, rehydroxylation proceeded more rapidly the higher the temperature and pressure, up to a particular temperature (Figure 1) above which hydralsite, pyrophyllite, and, in some runs, smectite began to form. The temperature at which rehydroxylation of metakaolinite was most rapid varied with pressure, from 270°C at 300 psi to 365°C at 30,000 psi (Figure 2). The temperature limit of stable kaolinite is 287°C at 5000 psi and 293°C at 20,000 psi, as shown below. Metastable kaolinite formed readily during the rehydroxylation of metakaolinite at higher temperatures, when the fluid was undersaturated with respect to quartz.

How the reaction products obtained from a charge of metakaolinite + water changed with temperature and pressure is shown in Figure 2. Left of the curve, kaolinite crystallized; to the right, hydralsite + pyrophyllite formed, their proportion increasing and that of initially formed kaolinite decreasing with increasing temperature. Increasing the reaction time from 7 days to several months shifted the upper part of this curve to the left and increased the proportion of pyrophyllite; thus, the curve is not an equilibrium stability curve. Above 400°C, andalusite appeared in one or two weeks, earlier at higher temperatures. A charge held at 420°C and 10,000 psi for a week transformed completely to hydralsite + pyrophyllite; if charges reacted under these conditions, unopened, were held another week at 10,000 psi, but each at a successively lower temperature, kaolinite first appeared at 290°C, as shown by runs along the arrow in Figure 2. Note that hydralsite did not form at pressures above the kyanite-andalusite boundary of Day and Kumin (1980).

The reaction products for a charge of metakaolinite + silica are shown in Figure 3. Each charge was 0.0828 g metakaolinite + 0.0828 ml H_2O + 0.0500 g silicic

https://doi.org/10.1346/CCMN.1985.0330101 Published online by Cambridge University Press

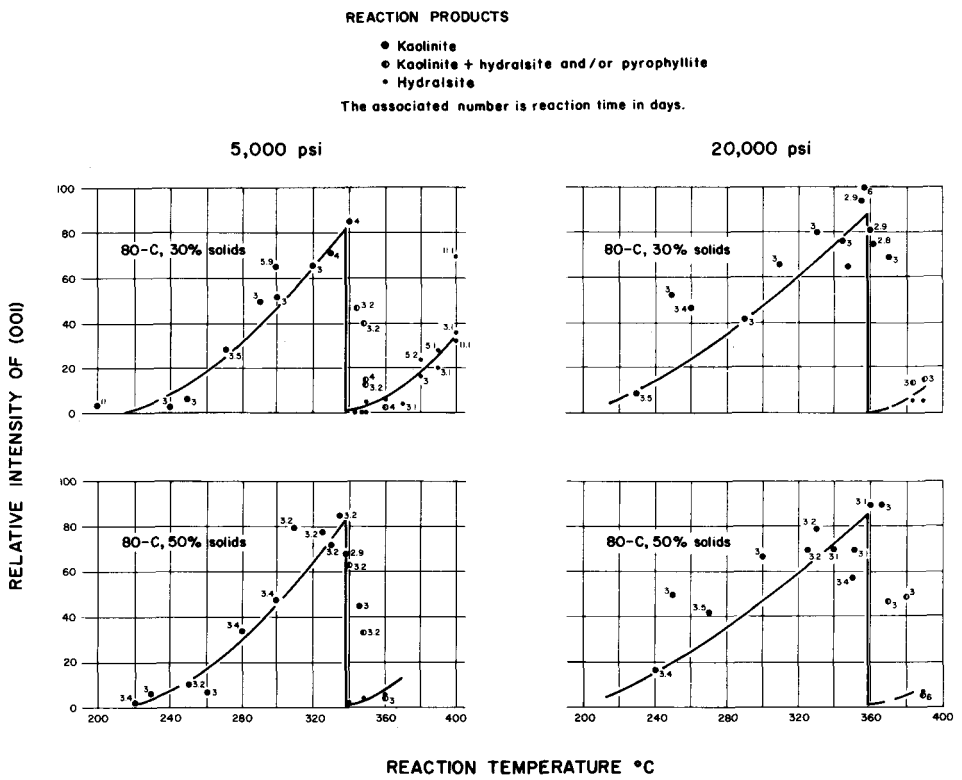

Figure 1. Basal spacings of rehydroxylation products of metakaolinite at 5000 and 20,000 psi water pressure. Rate of rehydroxylation increases with temperature up to the point at which other reaction products first appear.

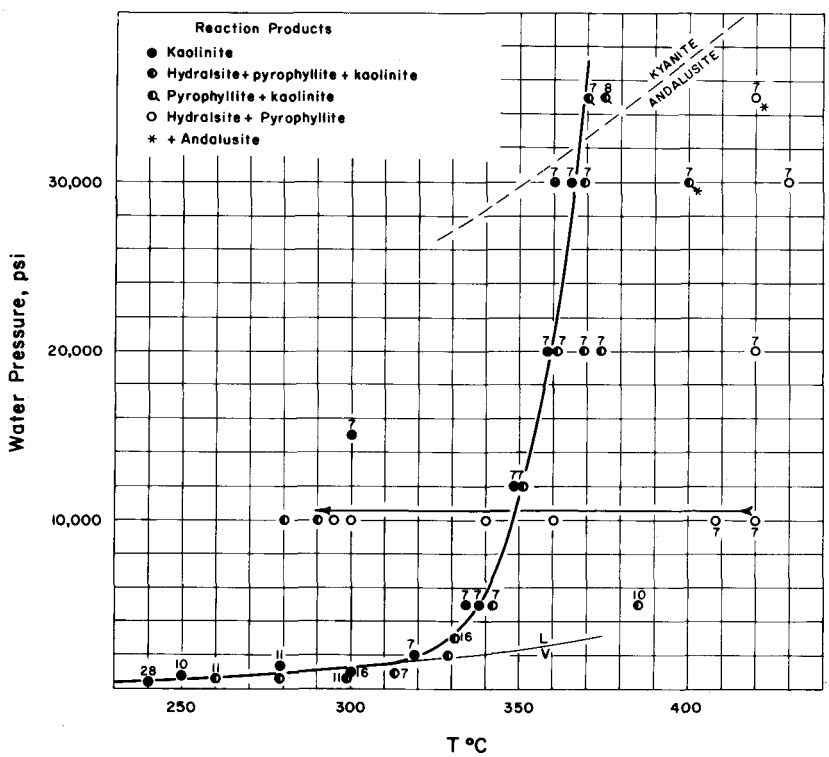

Figure 2. Reaction products from metakaolinite + water. Only kaolinite forms left of the curve. Numbers adjacent to symbols are the reaction times in days. The L/V curve is water's liquid-vapor curve. Runs along the arrow are explained in the text.

https://doi.org/10.1346/CCMN.1985.0330101 Published online by Cambridge University Press

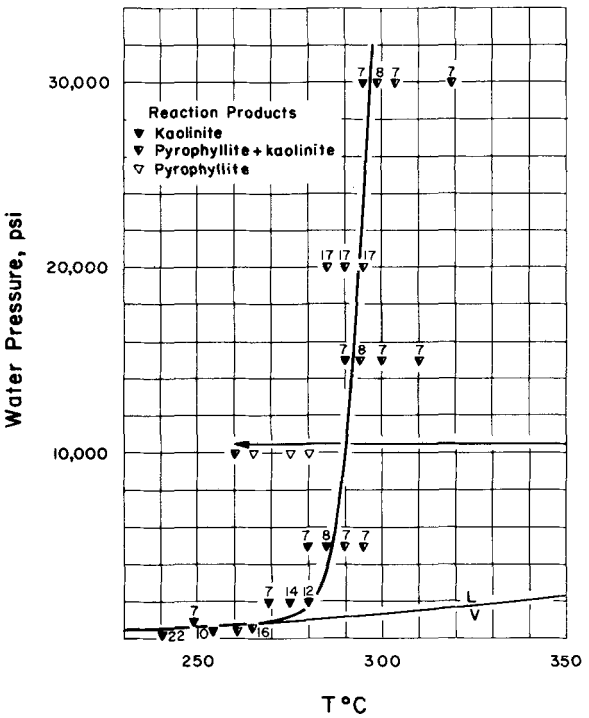

Figure 3. Reaction products from metakaolinite + silica + water. Only kaolinite forms left of the curve. Numbers adjacent to symbols are reaction times in days. The L/V curve is water's liquid/vapor curve. Runs along the arrow are explained in the text.

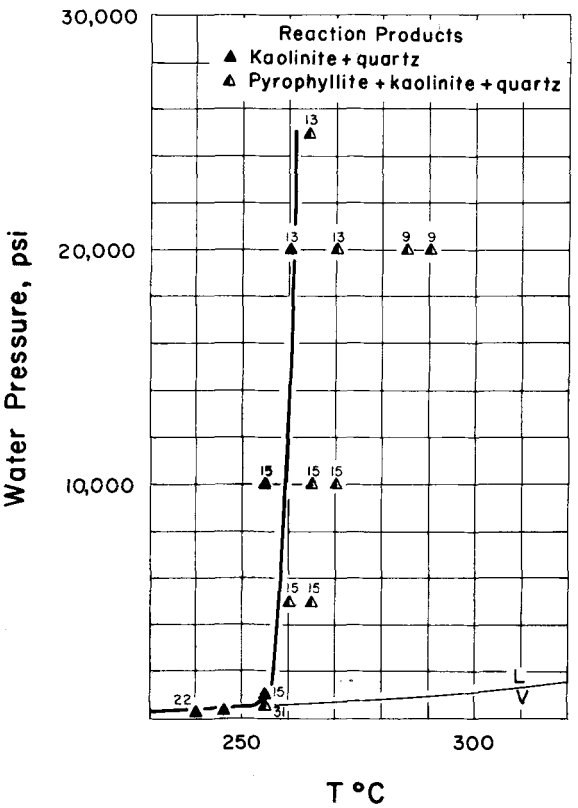

Figure 4. Reaction products from metakaolinite + silica + 20% HCl. This is a P-T diagram for the reaction Kaolinite + 2Quartz = Pyrophyllite + H_2O. Numbers adjacent to symbols are reaction times in days. The L/V curve is water's liquid-vapor curve.

acid containing 0.0448 g SiO_2. The added silica was just sufficient to convert all of the metakaolinite to pyrophyllite. To the left of the curve, kaolinite crystallized; to the right, pyrophyllite + kaolinite, the proportion of kaolinite decreasing with time. Hydralsite did not appear. Increasing reaction time shifted the upper part of the curve to the left, as seen in Figure 3, at 20,000 psi. When several charges held at 420°C and 10,000 psi for a week to transform the metakaolinite entirely to pyrophyllite were then cooled, unopened, at the same pressure to successively lower temperatures and held for another week, kaolinite first appeared at 260°C, as shown by runs along the arrow in Figure 3.

The reaction products for a charge of metakaolinite + silica + 20% HCl in the proportions above are shown in Figure 4. This charge ensured high activity of aqueous aluminum, principally $AlOH^{2+}$ (Helgeson, 1969), as well as aqueous silica, and therefore ensured rapid reaction. XRD patterns of the products show quartz in every run. The reaction products for a charge of natural kaolinite + water are shown in Figure 5. The upper part of this curve is similar to one determined by Roy and Osborn (1954).

Semilog plots of the data in Figures 2–4 reveal more

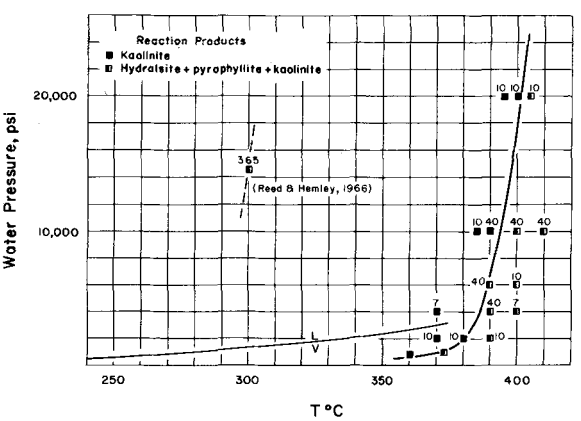

Figure 5. Non-equilibrium, hydrothermal dehydroxylation curve of kaolinite, the locus of P-T points at which reaction rate becomes sufficient to yield detectable products in 7–40 days. Numbers adjacent to symbols are reaction time in days. The L/V curve is water's liquid-vapor curve. Kaolinite's P-T-Time dehydroxylation curves mimic isopleths of water's free energy of formation.

https://doi.org/10.1346/CCMN.1985.0330101 Published online by Cambridge University Press

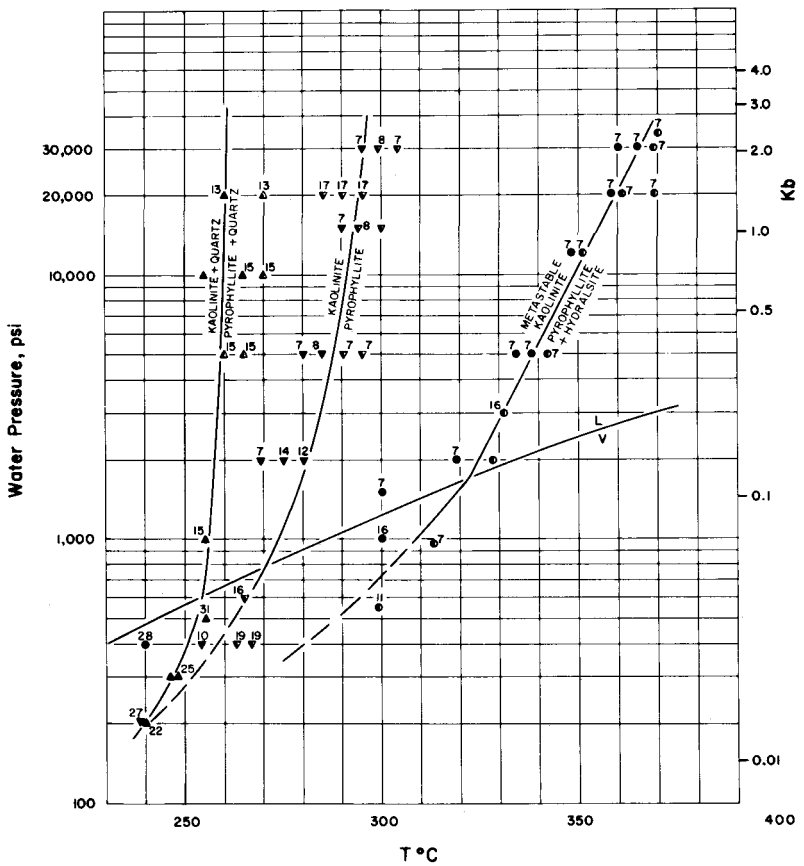

Figure 6. Semilog plots of the curves in Figures 2–4 show more clearly their behavior at lower pressures with respect to water's L/V curve.

clearly the behavior of the curves at lower pressures (Figure 6). Each curve changes slope below the L/V curve of water so as to parallel the isopleths of water's free energy of formation (see Helgeson and Kirkham, 1974, p. 1168).

Thermal dehydroxylation of kaolinite at atmospheric pressure

Typical thermal dehydroxylation curves for kaolinite (Figure 7) were obtained by heating small samples in air at fixed temperatures for a fixed time and measuring the XRD intensity of the 7.16-Å peak on pressed discs of the heated clay. The transformation to metakaolinite was attended by a decline in the XRD intensity of the 001 peak. The rate of dehydroxylation (negative slope of the curve) accelerated at about 400°C. Most samples were completely transformed at 600°C within a few minutes. An exception is the coarse and well-crystallized Keokuk kaolinite, whose differential thermogram shows an endothermic peak at 690°–695°C (Keller *et al.*, 1966). Even the Keokuk kaolinite dehydroxylated at <600°C over a 24-hr period.

DISCUSSION AND INTERPRETATION

Stability of kaolinite near atmospheric pressure

Below 200°C dehydroxylation of kaolinite was very slow, and the rate varied more with water vapor pressure than with temperature. For example, the thermogravimetric curves in Figure 1 of Achar *et al.* (1966) show that the extent of dehydroxylation at 300°C changes more from a 1-psi decrease in water vapor pressure than from a 100°C increase in temperature. Extrapolation of a semilog plot of the kaolinite + water curve of Figure 5 shows that 400 psi water pressure was sufficient to prevent dehydroxylation at 300°C. At 25°C, 0.46 psi water vapor pressure was sufficient to prevent dehydroxylation. In water-saturated rocks at temperatures left of the curve in Figure 4, kaolinite should therefore be stable unless it dissolves, as through low activity of H_4SiO_4, or reacts with dissolved species. In soils above the water table, where relative humidity may drop below 50% (Marshall, 1977), and at the earth's surface, kaolinite should dehydroxylate at a slow but measurable rate and therefore be unstable.

https://doi.org/10.1346/CCMN.1985.0330101 Published online by Cambridge University Press

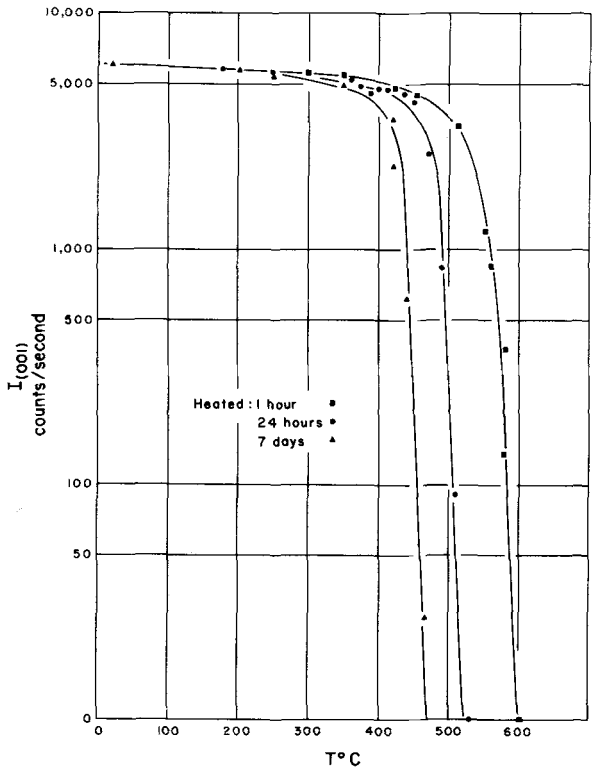

Figure 7. Typical thermal dehydroxylation curves for kaolinite. Rio Capim kaolinite heated in air. Intensities are from X-ray powder diffractograms.

Stability field of kaolinite

In the system Al_2O_3-SiO_2-H_2O, the stability field of kaolinite (Figures 8 and 9) is bounded by three isobaric univariant curves corresponding to the following hydroxylation-desilication reactions:

(1) Pyrophyllite + $5H_2O$ = Kaolinite + $2H_4SiO_4$
(2) Kaolinite + $3H_2O$ = 2Diaspore + $2H_4SiO_4$
(3) Kaolinite + $5H_2O$ = 2Gibbsite + $2H_4SiO_4$

Two isobaric invariant points are fixed by thermal dehydroxylation-silication reactions:

(4) Gibbsite + Diaspore + $2H_4SiO_4$ = Kaolinite + $4H_2O$
(5) 2Kaolinite = Pyrophyllite + 2Diaspore + $2H_2O$

Two other invariant points relate to

(6) Kaolinite + 2Quartz = Pyrophyllite + H_2O
(7) Pyrophyllite = Andalusite + 3Quartz + H_2O

Five additional curves shown in Figures 8 and 9 correspond to the reactions

(8) Pyrophyllite + $5H_2O$ = Andalusite + $3H_4SiO_4$
(9) Andalusite + $3H_2O$ = 2Diaspore + H_4SiO_4
(10) Pyrophyllite + $8H_2O$ = 2Diaspore + $4H_4SiO_4$
(11) 2Diaspore = Corundum + H_2O
(12) Gibbsite = Diaspore + H_2O

All of these reactions except the last two depend upon $[H_4SiO_4]$. The calculation of curves to represent these reactions requires reliable values for the free energy of formation of H_4SiO_4, which can be derived from the free energy of formation of water (Fisher and Zen, 1971; Hass, 1970), the free energy of formation and molar volume of quartz (Robie *et al.*, 1979), and the solubility of quartz.

The solubility of quartz repeatedly has been measured (Kennedy, 1944; Morey *et al.*, 1962; Siever, 1962; Anderson and Burnham, 1965; Crerar and Anderson, 1971, and others). With an equation of state whose parameters were derived by regression of available quartz solubility data, Walther and Helgeson (1977) calculated the solubility of aqueous silica to 5 kb and 600°C. More recent measurements by Hemley *et al.* (1980) agree closely with the 1 kb values of Walther and Helgeson (1977), though less well with their values for H_2O L/V pressures. Walther and Helgeson's values were used to plot the quartz saturation curves in Figures 8 and 9 and to calculate the free energy of formation of H_4SiO_4 (Table 2) because they yielded slightly better consistency between calculated curves and experimental points.

Interpretation of experimental curves

When kaolinite + water charges were heated, the initial reaction was incongruent dissolution. H_4SiO_4 increased rapidly at first but slowed as the fluid reacted with silica-depleted surfaces; H_4SiO_4 remained below quartz saturation for days. When silica was added, H_4SiO_4 increased and pyrophyllite began to form. Without added silica, H_4SiO_4 remained below curve (1) in Figures 8 and 9. When P-T conditions were to the right of kaolinite's stability field, kaolinite underwent no apparent change for weeks unless conditions were also to the right of the curve in Figure 5, which is a non-equilibrium, hydrothermal dehydroxylation curve. This curve gives the P-T point at which the reaction rate became great enough to yield detectable products in 7–40 days. The rate decreased with decreasing temperature, a year being required for detectable products to form at 300°C (Reed and Hemley, 1966).

When a high-solids mix of metakaolinite + water was heated within the P-T range of kaolinite's stability field, aqueous silica rose quickly to a value between curves (1) and (2) (Figures 8 and 9) and kaolinite began to recrystallize. At higher temperatures but still below the stability field of andalusite, aqueous silica remained along curve (10); a small increase in aqueous silica triggered growth of pyrophyllite, but an increase in aqueous Al caused boehmite to form. At higher tem-

https://doi.org/10.1346/CCMN.1985.0330101 Published online by Cambridge University Press

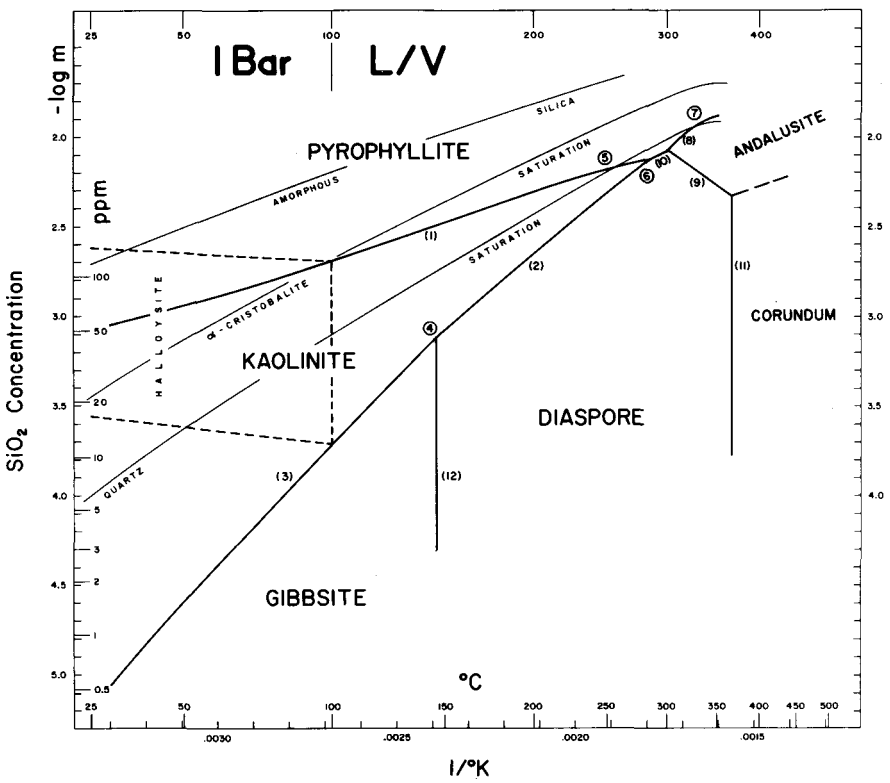

Figure 8. Stability field of kaolinite in the system Al_2O_3-SiO_2-H_2O along the liquid-vapor curve, down to 1 bar. For temperatures of isobaric invariant points see Table 1. How point "5" shifts with pressure is shown by the curve in Figure 4. How points "6" and "7" shift with pressure is closely approximated by the curves in Figures 3 and 2, respectively.

peratures up to point "7," aqueous silica must remain near curve (8), tending to rise above it, because very slow growth of pyrophyllite became detectable after several weeks. Adding a little silica caused rapid formation of pyrophyllite. At point "7," where the quartz saturation curve intersects curve (8), pyrophyllite + hydralsite formed rapidly in place of metastable kaolinite.

Many runs showed that hydralsite crystallized only within the andalusite field. At temperatures to the right of point "7," aqueous silica remained along curve (8), with initial crystallization of pyrophyllite + metastable hydralsite and a final stable assemblage of pyrophyllite + andalusite + quartz.

Figure 2 shows how the temperature of point "7" changed with pressure. When a charge that had completely transformed to pyrophyllite + hydralsite was held at successively lower temperatures, aqueous silica dropped to its equilibrium value on the ordinate at that temperature, along curves (8) and (10), and the ratio pyrophyllite:hydralsite increased until the temperature of point "6" was reached, when kaolinite began to crystallize. This reaction is shown by runs along the arrow in Figure 2 which indicate the same temperature for point "6" approached from higher temperature as indicated by Figure 3, where point "6" was approached from lower temperature.

When a high-solids mix of metakaolinite + water + sufficient silica to convert metakaolinite to pyrophyllite was heated within the P-T range of kaolinite's stability field, aqueous silica rose quickly to a value between curves (1) and (2) and kaolinite began to recrystallize. Up to the temperature of point "5" (Figures 8 and 9), only kaolinite was quick to crystallize, though quartz was detectable after a few days. At temperatures between points "5" and "6," aqueous silica was buffered at first by crystallizing kaolinite but rose during a 1–2 week period above curve (1) and pyrophyllite began to form. Thus, the curve in Figure 3 shifted a little to the left when run time exceeded one week. For short runs at temperatures up to point "6," only kaolinite was detectable by X-rays. At temperatures above point "6," pyrophyllite formed. When a charge that was completely transformed to pyrophyllite + quartz was held at successively lower temperatures, aqueous silica decreased along the quartz saturation curve until the temperature of point "5" was reached, whereupon kaolinite began to crystallize. Runs along the arrow in Figure

https://doi.org/10.1346/CCMN.1985.0330101 Published online by Cambridge University Press

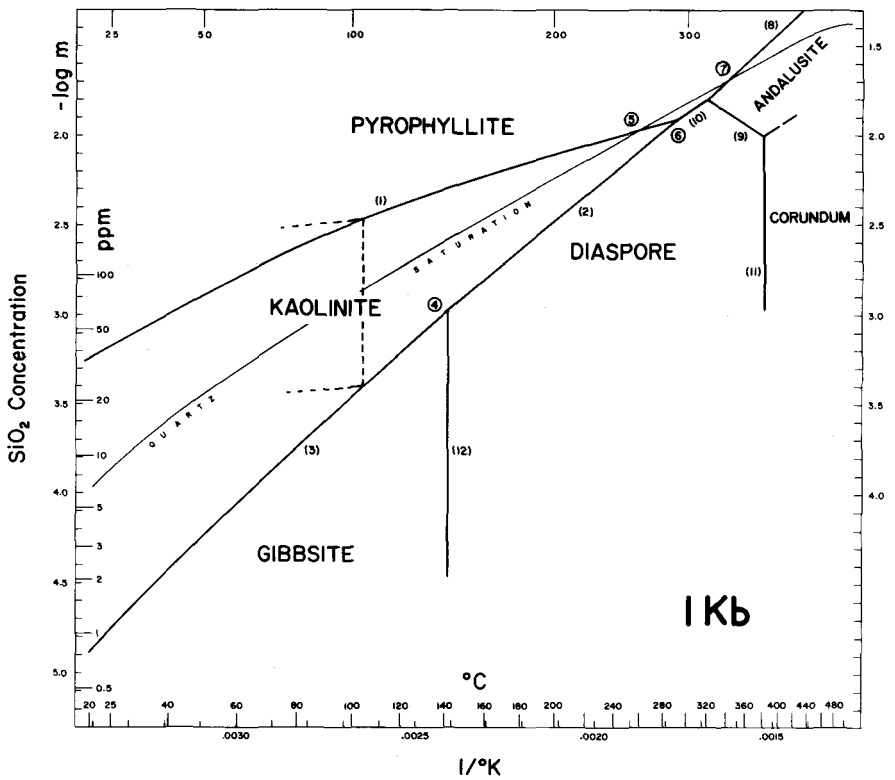

Figure 9. Stability field of kaolinite in the system Al_2O_3-SiO_2-H_2O at 1 kb water pressure. For temperatures of isobaric invariant points, see Table 1.

3 gave the same temperature for point "5" approached from higher temperature as indicated by Figure 4, where point "5" was approached from lower temperature.

When a high-solids mix of metakaolinite + silica + 20% HCl was heated at a temperature below point "5," a little boehmite crystallized at first, the activity of aqueous Al being very high, but soon the concentration of aqueous silica rose to a value within the stability field of kaolinite, which began to crystallize. After a week the reaction product showed a trace of quartz, as seen in Figure 4. At a temperature slightly to the right of point "5" pyrophyllite began to form. In the reverse direction, pyrophyllite + quartz began to transform to kaolinite + quartz near the temperature of point "5." The temperature interval over which this transformation was reversible in 2 weeks was 5°C. How the temperature of point "5" varied with pressure is seen in Figure 4.

Synthesis field of hydralsite

Since first described by Roy and Osborn (1954), hydralsite has been mentioned in several reports on the Al_2O_3-SiO_2-H_2O system (Aramaki and Roy, 1963; Velde and Kornprobst, 1969), though not in others (Carr and Fyfe, 1960; Hemley *et al.*, 1980). More than 200 hydrothermal runs show a restricted range of conditions wherein hydralsite formed and a clear trend for its disappearance with increasing reaction time, as equilibrium was approached.

Hydralsite is a fast-forming, metastable phase that crystallized in lieu of andalusite when the activity of aluminum was low, particularly when the fluid was undersaturated with respect to quartz. In no experiment was it seen to form outside the stability field of andalusite, nor above 560°C. Hydralsite should be expected in nature only where composition approximated the Al_2O_3-SiO_2-H_2O system, aqueous aluminum was low, H_4SiO_4 was $\sim 10^{-1.5}$–$10^{-2.4}$, temperature ~300°–560°C and not long maintained, and pressure was below the kyanite-andalusite boundary. A natural occurrence has not been reported.

Calculation of the stability field of kaolinite

Invariant point "5" in Figure 8 is the intersection of curve (1), representing reaction (1), Pyrophyllite + $5H_2O$ = Kaolinite + $2H_4SiO_4$, with the quartz saturation curve. The experimentally determined temperature of this point is 260°C (Table 1) corresponding to an aqueous silica value of $10^{-1.97}$. The standard free energy change of reaction (1) is

https://doi.org/10.1346/CCMN.1985.0330101 Published online by Cambridge University Press

$$\Delta G^0_{(T,1\ kb)} = G^0_f Kaol._{(298,1\ b)} + 2G^*_f H_4SiO_{4(T,1\ kb)} - G^0_f Pyrophy._{(298,1\ b)} - 5G^*_f H_2O_{(T,1\ kb)} + \Delta V_s \Delta P - \Delta S^0_{(f,s)} \Delta T + \int_{298}^{T} \Delta Cp_{(f,s)} dT - \int_{298}^{T} \Delta Cp_{(f,s)} d \ln T$$

(Hemley *et al.*, 1980),

where G^0_f is the standard molar free energy of formation of the solids from the elements, G^*_f is the standard Gibbs free energy (Fisher and Zen, 1971), ΔV_s is the volume change of reaction for the solids at 298°K, 1 bar, $\Delta S^0_{f,s}$ is the change in entropy of formation of the solids at 298°K, and $\Delta Cp_{f,s}$ is the change in heat capacity of formation of the solids. At T = 533.15°K and 1 kb, here chosen as the reference state, the standard free energy change of reaction (1) is $2RT \ln 10^{1.97}$. The solution of the equation, after substituting requisite data from Tables 2 and 3, is a numerical value for $G^0_f Kaol._{(298,1\ b)} - G^0_f Pyrophy._{(298,1\ b)}$, 1,467,573 J. This value is only 1053 J more than the difference shown by Robie *et al.* (1979).

Solving the above equation at T = 566.15°K, the experimental value for point "6," gives an aqueous silica value of $10^{-1.92}$ and thus defines a point on curve (2). A similar thermodynamic equation for reaction (2) gives G^0_f(Diaspore) with respect to G^0_f(Kaol.).

Of the three equations representing curves (1), (2), and (8), the element G^0_f(Kaol.) is common to curves (1) and (2), and G^0_f(Pyrophy.) is common to curves (1) and (8). Computer-assisted trial solutions of these equations, varying the values of common elements, were used to find values consistent with all geometric and experimental constraints for the standard Gibbs free energy of formation of kaolinite, pyrophyllite, andalusite, and diaspore.

The experimental data enabled calculation of the difference between two G^0_f values in each of three cases. G^0_f(Kaol.) appeared to have been well evaluated by previous work (Barany and Kelley, 1961; Hemingway *et al.* (1978). The trial solutions showed that any increase or decrease in the Hemley *et al.* (1980) value would generate inconsistency between experimental data and calculated curves. The Hemley *et al.* value for G^0_f(Kaol.) therefore was taken as the absolute reference, and other G^0_f values were evaluated with respect to it (Table 3).

Invariant point "4" representing reaction (4) was approximated by plotting the intersection of two curves: (a) temperature vs. $G^*_f H_4SiO_4$ from Table 2, and (b) temperature vs. $\Delta G^*_f H_4SiO_4$ derived from the equation $2\Delta G^*_f H_4SiO_{4(T,P)} = \Delta G_f Kaol._{(T,P)} + 4\Delta G^*_f H_2O_{(T,P)} - \Delta G_f Gibbsite_{(T,P)} - \Delta G_f Diaspore_{(T,P)}$. The resulting value was higher than the 100°C mentioned by Wefers and Bell (1972) and 9°C lower than the experimental approximation of 155°C by Laubengayer and Weisz (1943).

All slanting curves in Figures 8 and 9 were calculated from data in Table 3 and Robie *et al.* (1979). Curve (11) is from Fyfe and Hollander (1964). Curve (12) was located as outlined above. The dashed vertical curve was approximated from published data, reviewed below.

Stability field of halloysite

When rocks differing widely in composition are subjected to weathering (Parham, 1969) or low-temperature hydrothermal alteration, halloysite is a common alteration product. It may form as the principal secondary mineral or in association with kaolinite or smectite, depending upon the activity of H_4SiO_4 and alkaline earths (Busenberg, 1978). If water pressure drops below L/V pressures, halloysite tends to dehydrate irreversibly to metahalloysite.

The halloysite-kaolinite phase boundary, a vertical line in Figures 8 and 9, can be approximated from published data. Roy and Osborn (1954) reported that halloysite is stable at water's L/V pressures up to 170°C; above this temperature it dehydrates at all pressures up to 30,000 psi. Their criterion for stability, whether any halloysite remained after hydrothermal treatment, did not allow for reaction kinetics, hence their maximal temperature for stable halloysite is too high. Minato and Aoki (1979) detected no dehydration at 100°C and 120°C but rapid dehydration at 135°C, at L/V pressures. Their dehydration rate curves indicate that halloysite dehydrates in longer runs well below 120°C. The

Table 1. Temperatures (°C) of isobaric invariant points in Figures 8 and 9.

	This study		Hemley *et al.* (1980)		Other		
Point	L/V	1 kb	L/V	1 kb	L/V	1 kb	
4	146	142			155		Laubengayer and Weisz (1943)
5	254	260 ± 2		273 ± 10			
6	284	293 ± 2		300 ± 10			
7	335	355 ± 2		366 ± 10		360	Haas and Holdaway (1973)
Intersection (9) and (11)			370 ± 10	394 ± 10	360 ± 7		Fyfe and Hollander (1964)
						384	Haas (1972)

https://doi.org/10.1346/CCMN.1985.0330101 Published online by Cambridge University Press

Table 2. Gibbs free energy of formation (Joules/mole of H_2O and H_4SiO_4.

T (°C)	$G^*_fH_2O$ L/V[1]	1 kb[2]	−log m H_4SiO_4 L/V pressure of H_2O	$G^*_fH_4SiO_4$	−log m H_4SiO_4 1 kb	$G^*_fH_4SiO_4$
440		−173,565			−1.450	−1,105,842
420		−176,289			−1.491	−1,114,907
400		−179,042			−1.534	−1,124,023
380		−181,828			−1.581	−1,133,202
360		−184,640			−1.635	−1,142,388
340	−189,606	−187,460	−1.919	−1,155,168	−1.692	−1,151,603
320	−192,432	−190,326	−1.953	−1,164,872	−1.758	−1,160,857
300	−195,313	−193,217	−2.011	−1,174,430	−1.827	−1,170,184
280	−198,187	−196,095	−2.079	−1,183,911	−1.900	−1,179,507
260	−201,150	−199,033	−2.153	−1,193,556	−1.973	−1,188,997
240	−204,003	−201,974	−2.236	−1,202,951	−2.057	−1,198,352
220	−206,946	−204,937	−2.329	−1,212,479	−2.148	−1,207,959
200	−209,916	−207,949	−2.427	−1,222,093	−2.243	−1,217,592
180	−212,904	−210,957	−2.536	−1,231,720	−2.350	−1,227,193
160	−215,924	−213,999	−2.651	−1,241,446	−2.467	−1,236,863
140	−218,982	−217,062	−2.783	−1,251,193	−2.593	−1,246,600
120	−222,057	−220,158	−2.931	−1,260,960	−2.737	−1,256,358
100	−225,167	−223,267	−3.095	−1,270,793	−2.906	−1,266,077
80	−228,313	−226,306	−3.273	−1,280,729	−3.094	−1,275,658
60	−231,304	−229,601	−3.497	−1,290,196	−3.323	−1,285,631
40	−234,709	−232,883	−3.747	−1,300,501	−3.604	−1,295,438
20	−237,961	−236,152	−4.090	−1,310,167	−3.945	−1,305,094

$G^*_fH_4SiO_4$ calculated from quartz solubilities of Walther and Helgeson (1977), free energy of formation and molar volume of quartz from Robie *et al.* (1979) and the $G^*_fH_2O$ values shown on the left.

[1] From the fugacity data of Hass (1970).

[2] >100°C from Fisher and Zen (1971); <100°C, from Robie *et al.* (1979).

Table 3. Thermochemical data, 25°C, 1 bar.

	G^0_f (J/gf)	S^0 (J/deg gf)[1]	S^0_f (J/deg gf)[1]	V (J/bar gf)[1]	Cp[3] a	b	c	d
Kaolinite	−3,799,364[1] ± 2.6	203.0 ± 1.3	−1075.855 ± 1.33	9.9521	6.1600	−523.606	0	−61.4224
Pyrophyllite	−5,266,937[2]	239.40 ± 0.40	−1254.121 ± 0.60	12.590	10.4692	−2201.80	39.8120	−126.339
Diaspore	−920,267[2]	35.338 ± 0.17	−263.502 ± 0.25	1.775	1.4720	0	1.548	−16.490
Quartz	−856,288[1]	41.46 ± 0.20	−182.500 ± 0.20	2.2688	0.8325	219.68	0	−7.7798
Gibbsite	−1,154,889[1]	68.44	−463.655	3.1956		(G^0_f available for 127°C)		
Andalusite	−2.442,300[2]	93.22	−495.165	5.153	3.3244	−275.28	1.2379	−35.033
Al	0	28.35	0	0.9999	27.237	−65.674	−1.9916	0***
O_2	0	205.15	0	2446.50	0.4832	−6.9132	4.9923	−4.2066
H_2	0	130.68	0	2459.05	0.0744	117.07	−5.1041	4.1017**
Si	0	18.81	0	1.2056	0.3178	5.3878	−1.4654	−1.7864

[1] Robie *et al.* (1978).

[2] This study.

All unreferenced values are from Hemley *et al.* (1980).

[3] $Cp = a10^2 + b10^{-4}T + c10^5T^{-2} + d10^2T^{-1/2} + e10^{-5}T^2$.

$\int_{T_1}^{T_2}\Delta Cp_{f,s}dT = \Delta a10^2\Delta T + (\Delta b/2)10^{-4}(T_2^2 - T_1^2) - \Delta c10^5(1/T_2 - 1/T_1) + 2\Delta d10^2(T_2^{1/2} - T_3^{1/2}) + (\Delta e/3)10^{-5}(T_2^3 - T_1^3)$.

$\int_{T_1}^{T_2}\Delta Cp_{f,s}d \ln T = \Delta a \ln T_2/T_1 + \Delta b10^{-4}\Delta T - \Delta c/2(10^5)(1/T_2^2 - 1/T_1^2) - 2\Delta d10^2(1/T_2^{1/2} - 1/T_1^{1/2}) + \Delta e/2(10^{-5})(T_2^2 - T_1^2)$.

** e = −0.139.

*** e = 1.431.

https://doi.org/10.1346/CCMN.1985.0330101 Published online by Cambridge University Press

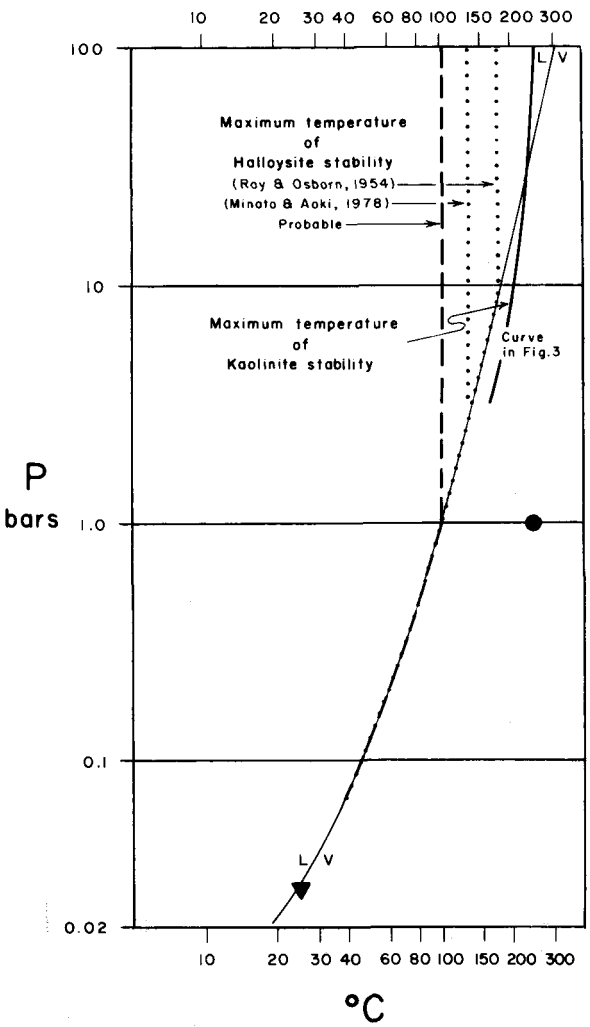

Figure 10. Maximum temperatures for halloysite and kaolinite stability at low water pressures. The triangle marking rapid dehydration of halloysite is from Hughes (1966). The solid circle marking onset of rapid dehydroxylation of kaolinite is from Figure 7.

water pressure at which dehydration commences is approximated by the L/V curve very closely up to 100°C; at higher pressures the temperature remains below ~110°C, as indicated in Figure 10.

One position of the pyrophyllite-halloysite and halloysite-gibbsite boundaries at 25°C can be calculated from data in Robie *et al.* (1979). These boundaries are at higher silica activities than the pyrophyllite-kaolinite and kaolinite-gibbsite boundaries because the Gibbs free energy of formation of halloysite is slightly higher. Decreasing crystallinity of halloysite, other factors being equal, pivots these boundaries clockwise about their intersection near 100°C with the pyrophyllite-kaolinite and kaolinite-gibbsite lines. Increasing disorder in kaolinite shifts its phase boundaries upward, while improved growth conditions for halloysite leading to higher order and lower free energy shifts its boundaries downward, toward coincidence with those of kaolinite.

Below 100°C, either halloysite or kaolinite may form. High H_4SiO_4, the presence of elements that may substitute for Si and Al, fluctuating conditions—whatever favors rapid growth, disorder, and interlayer water—should favor the formation of halloysite. These arguments are consistent with Keller's conclusion (1978), based upon a scanning electron microscopic study of weathered products throughout the world, that halloysite is characteristic of near-surface or highland areas where weathering conditions are transitory, whereas kaolinite is more characteristic of thick saprolitic zones where conditions have persisted, perhaps near equilibrium, for long periods.

Below 100°C, at all water pressures greater than L/V pressures, halloysite's interlayer water should remain intact, even though continued interaction with the pore fluid may improve order and eliminate any initial layer charge deficiency. Halloysite can recrystallize readily at low temperature when the composition of the pore fluid is suitable (La Iglesia and Galan, 1975), when aqueous aluminum is high. Upon exposure to soil air of moderate humidity or the atmosphere, halloysite tends to lose its interlayer water irreversibly, the rate of loss being particularly sensitive to water pressure and less sensitive to particle size. The transformation to metahalloysite, often hard to distinguish from kaolinite, is rapid in the upper part of even immature weathering profiles (Kremer, 1983). Dehydration may result from simple desiccation or dehydration coupled with recrystallization, apt to be accompanied by a morphological change. Above ~110°C, halloysite tends to transform to kaolinite at any water pressure.

The prevalence of halloysite where silica activity is high, as in glassy volcanic rocks that have been subjected to weathering or low-temperature hydrothermal alteration, has been noted many times. Also frequently noted in the literature is the association of kaolinite with gibbsite where silica activity is low. Where halloysite and kaolinite are zonally associated, the kaolinite zone is in the direction of higher temperature of formation. These associations, often observed, are consistent with stability relations as derived in Figures 8 and 9. The overlap of formational conditions and the ease with which halloysite may transform to kaolinite contribute to the difficulty commonly encountered in differentiating these minerals.

CONCLUSIONS

The maximal temperature for stable kaolinite is about 300°C, decreasing from 296°C at 2 kb water pressure to 284°C at water's L/V pressure, and decreasing very rapidly at lower pressures (Figure 3). On an isobaric plot of $[H_4SiO_4]$ vs. $°K^{-1}$, kaolinite's wedge-shaped sta-

https://doi.org/10.1346/CCMN.1985.0330101 Published online by Cambridge University Press

bility field (Figures 8 and 9) broadens toward lower temperatures to include much of the range of aqueous silica in near-surface environments. This range generally is <1 ppm to ~40 ppm (McKeague and Cline, 1963, in Kittrick, 1969) but may exceed 100 ppm. Where $[H_4SiO_4]$ is above kaolinite's stability field, halloysite tends to form rather than pyrophyllite. Though pyrophyllite is common in some sediments and soils, no clear case of its origin through pedogenesis has been described. According to Figure 8, pedogenic pyrophyllite should be rare; hydrothermal pyrophyllite, on the other hand, should form readily where $[H_4SiO_4]$ is controlled by cristobalite or noncrystalline silica, at temperatures as low as 150°C.

The de- and re-silication reactions that bound kaolinite's stability field are relatively fast. During experiments on the artificial weathering of feldspars, Busenberg (1978) found that all solutions reached equilibrium with fine-grained reaction products within 100 hr at 25°C. When these reactions hardly proceed, the usual reason is low activity of aqueous aluminum or buffering of $[H_4SiO_4]$ at a value precluding change.

Despite continuing attempts to portray kaolinite stability on a P-T plot (Minato *et al.*, 1982), a third variable, at least, must be defined. Aqueous silica is a preferred variable because, unlike aqueous aluminum, it exists essentially as one species having relatively high activity over the pressure-pH range of most low-temperature natural environments.

Kaolinite is a characteristic mineral of low- to moderate-temperature, low-pH, high-Eh, low-alkali, intermediate-H_4SiO_4 environments, as indicated by Figures 8 and 9, the activity-activity diagrams of Bricker *et al.* (1968) and Marshall (1977), and the common observation that kaolinite is better crystallized where the iron in the system is tied up in ferric minerals. Where log $pH[K^+,Na^+,Mg^{2+}] > 3$, smectite may form. Where log $pH[K^+] > 5$, illite may form in lieu of kaolinite. Log $pH[Na^+] > 6$ allows the formation of a zeolite phase. Progressive leaching of alkalies and alkaline earths, under oxidizing conditions, transforms smectite and other silicates to kaolinite. This transformation is almost ubiquitous in saprolites that have smectite deep in the profile. In anaerobic environments, where Eh < +100 mV, released iron is apt to be ferrous, highly mobile, and may be incorporated substitutionally in kaolinite (Bhattacharyya, 1983), unless there is sufficient sulfur to immobilize the iron as pyrite.

The formation of halloysite is favored by high H_4SiO_4 and conditions that favor substitutional impurities. It may persist so long as water pressure remains above L/V pressures and temperature below ~100°C.

Hydralsite is a fast-forming metastable phase. In experiments described here, it formed only within the pressure-temperature range of andalusite's stability field. No natural occurrence has been reported.

Most kaolinite and halloysite have been produced by weathering. Kaolinite has survived as a common constituent of sediments ranging in age from Devonian to Present. Much less halloysite has survived, due to its low dehydration temperature and instability at low water pressures. Kaolinite commonly is a dominant mineral in lacustrine and fluviatile deposits. It is abundant in oxidized sediments and in reduced marine sediments when they are pyritic. In buried sediments, the $[H_4SiO_4]$ and water pressure required for kaolinite stability commonly have been maintained and kaolinite has tended to survive, but where alkalies, alkaline earths, or aqueous iron have concentrated in the pore fluid, kaolinite has tended to transform to illite, zeolites, berthierine, or other minerals.

ACKNOWLEDGMENTS

Thomas Kremer drafted the figures. Willis B. Hayes assisted with computer programming. Allen D. King, Jr. and C. R. Price gave valuable comments and suggestions. Most of the work was supported by the J. M. Huber Corporation. The authors especially thank J. J. Hemley for a critical review of the manuscript.

REFERENCES

Achar, N. N., Brindley, G. W., and Sharp, J. H. (1966) Kinetics and mechanism of dehydroxylation processes, III. Applications and limitations of dynamic methods: in *Proc. Int. Clay Conf. Jerusalem,* 1966, **1,** L. Heller and A. Weiss, eds., Israel Prog. Sci. Transl., Jerusalem, Israel, 67–73.

Anderson, G. M. and Burnham, C. W. (1965) The solubility of quartz in supercritical water: *Amer. J. Sci.* **263,** 494–511.

Aramaki, Shigeo and Roy, Rustum (1963) A new polymorph of Al_2SiO_5 and further studies in the system Al_2O_3-SiO_2-H_2O: *Amer. Mineral.* **48,** 1322–1347.

Barany, R. and Kelley, K. K. (1961) Heats and free energies of formation of gibbsite, kaolinite, halloysite, and dickite: *U.S. Bur. Mines Rept. Inv.* **5825,** 1–13.

Bhattacharyya, D. P. (1983) Origin of berthierine in ironstones: *Clays & Clay Minerals* **31,** 173–182.

Bricker, O. P., Godfrey, A. E., and Cleaves, E. T. (1968) Mineral-water interaction during the chemical weathering of silicates: in *Trace Inorganics in Water,* R. F. Gould, ed., Advances in Chem. Ser., **73,** Amer. Chem. Soc., Washington, D.C., 128–142.

Busenberg, Eurybiades (1978) The product of the interaction of feldspars with aqueous solutions at 25°C: *Geochim. Cosmochim. Acta* **42,** 1679–1686.

Carr, R. M. and Fyfe, W. S. (1960) Synthesis fields of some aluminum silicates: *Geochim. Cosmochim. Acta* **21,** 99–109.

Crerar, D. A. and Anderson, G. M. (1971) Solubility and solvation reactions of quartz in dilute hydrothermal solutions: *Chem. Geology* **8,** 107–122.

Day, H. D. and Kumin, H. J. (1980) Thermodynamic analysis of the aluminum silicate triple point: *Amer. J. Sci.* **280,** 265–287.

von Dietzel, A. and Dhekne, B. (1957) Über die Rehydratation von Metakaolin: *Ber. Deut. Keram. Ges.* **34,** 366–377.

Eberl, D. D. and Hower, J. (1975) Kaolinite synthesis: the role of the Si/Al and (alkali)/H^+ ratio in hydrothermal systems: *Clays & Clay Minerals* **23,** 301–309.

Fisher, J. R. and Zen, E-An (1971) Thermochemical calculations from hydrothermal phase equilibrium data and the free energy of H_2O: *Amer. J. Sci.* **270,** 297–314.

Fyfe, W. S. and Hollander, M. A. (1964) Equilibrium dehydration of diaspore at low temperature: *Amer. J. Sci.* **262,** 709–712.

Garrels, R. M. and Christ, C. L. (1965) *Solutions, Minerals, and Equilibria:* Harper and Row, New York, 450 pp.

Haas, Herbert (1972) Diaspore-corundum equilibrium determined by epitaxis of diaspore on corundum: *Amer. Mineral.* **57,** 1375–1385.

Haas, Herbert and Holdaway, M. J. (1973) Equilibrium in the system Al_2O_3-SiO_2-H_2O involving the stability limits of pyrophyllite and thermodynamic data of pyrophyllite: *Amer. J. Sci.* **273,** 449–464.

Hass, J. L., Jr. (1970) Fugacity of H_2O from 0° to 350°C at the liquid-vapor equilibrium and at 1 atmosphere: *Geochim. Cosmochim. Acta* **34,** 920–932.

Helgeson, H. C. (1969) Thermodynamics of hydrothermal systems at elevated temperatures and pressures: *Amer. J. Sci.* **267,** 729–804.

Helgeson, H. C. and Kirkham, D. H. (1974) Theoretical prediction of the thermodynamic behavior of aqueous electrolytes at high pressures and temperatures: I. Summary of the thermodynamic/electrostatic properties of the solvent: *Amer. J. Sci.* **274,** 1089–1198.

Hemingway, B. S., Robie, R. A., and Kittrick, J. A. (1978) Revised values for the Gibbs free energy of formation of $Al(OH)_4$ aq., diaspore, boehmite, and bayerite at 298.15°K and 1 bar, the thermodynamic properties of kaolinite to 800°K and 1 bar, and the heats of solution of several gibbsite samples: *Geochim. Cosmochim. Acta* **42,** 1533–1554.

Hemley, J. J. (1959) Some mineralogical equilibria in the system K_2O-Al_2O_3-SiO_2-H_2O: *Amer. J. Sci.* **257,** 241–270.

Hemley, J. J., Montoya, J. W., Marinenko, J. W., and Luce, R. W. (1980) Equilibria in the system Al_2O_3-SiO_2-H_2O and some general implications for alteration/mineralization processes: *Econ. Geol.* **75,** 210–228.

Henley, R. W. (1973) Solubility of gold in hydrothermal chloride solutions: *Chem. Geol.* **11,** 73–87.

Hill, R. D. (1953) The rehydration of fired clay and associated minerals: *Trans. Brit. Ceram. Soc.* **52,** 589–613.

Hill, R. D. (1955) 14Å spacing in kaolin minerals: *Acta Crystallogr.* **8,** p. 120.

Hughes, I. R. (1966) Mineral changes of halloysite on drying: *N.Z. J. Sci.* **9,** 103–113.

Hurst, V. J. and Basio, N. J. (1975) Rio Capim kaolin deposits, Brazil: *Econ. Geol.* **70,** 990–992.

Keller, W. D., Pickett, E. E., and Reesman, A. L. (1966) Elevated dehydroxylation temperature of the Keokuk geode kaolinite—a possible reference mineral: in *Proc. Inter. Clay Conf. Jerusalem 1966,* **1,** L. Heller and A. Weiss, eds., Israel Prog. Sci. Transl., Jerusalem, Israel, 75–85.

Keller, W. D. (1978) Kaolinization of feldspars as displayed in scanning electron micrographs: *Geology* **6,** 184–188.

Kennedy, G. C. (1944) The hydrothermal solubility of silica: *Econ. Geol.* **39,** 25–36.

Kittrick, J. A. (1969) Soil minerals in the Al_2O_3-SiO_2-H_2O system and a theory of their formation: *Clays & Clay Minerals* **17,** 157–167.

Kremer, Thomas (1983) SEM and XRD investigation of mineralogical transformations during weathering: M.S. thesis, Univ. Georgia, Athens, Georgia, 115 pp.

La Iglesia, A. and Galan, E. (1975) Halloysite-kaolinite transformation at room temperature: *Clays & Clay Minerals* **23,** 109–113.

Laubengayer, A. W. and Weisz, R. S. (1943) A hydrothermal study of equilibria in the system alumina-water: *J. Amer. Chem. Soc.* **65,** 247–250.

Marshall, C. E. (1977) *The Physical Chemistry and Mineralogy of Soils:* Wiley-Interscience, New York, 313 pp.

McKeague, J. A. and Cline, M. G. (1963) Silica in soils: *Adv. Agron.* **15,** 339–396.

Minato, H. and Aoki, M. (1979) Rate of transformation of halloysite to metahalloysite under hydrothermal conditions: in *Proc. Inter. Clay Conf., Oxford, 1978,* M. M. Mortland and V. C. Farmer, eds., Elsevier, Amsterdam, 619–627.

Minato, Hideo; Kusakabee, Hirotatsu; and Inoue, Atsuyuki (1982) Alteration reactions of halloysite under hydrothermal conditions with acidic solutions: in *Proc. Int. Clay Conf., Bologna, Pavia, 1981,* H. van Olphen and F. Veniale, eds., Elsevier, Amsterdam, 565–571.

Morey, G. W., Fournier, R. O., and Rowe, J. J. (1962) The solubility of quartz in water in the temperature interval from 25°C to 300°C: *Geochim. Cosmochim. Acta* **26,** 1029–1043.

Parham, W. E. (1969) Formation of halloysite from feldspar: low temperature, artificial weathering versus natural weathering: *Clays & Clay Minerals* **17,** 13–22.

Reed, B. L. and Hemley, J. J. (1966) Occurrences of pyrophyllite in the Kekiktuk conglomerate, Brooks Range, Northeast Alaska: *U.S. Geol. Surv. Prof. Pap.* **550-C,** 162–166.

Robie, R. A., Hemingway, B. S., and Fisher, J. R. (1979) Thermodynamic properties of minerals and related substances at 298.15°K and 1 bar (155 Pascals) pressure and at higher temperatures: *U.S. Geol. Surv. Bull.* **1452,** 456 pp.

Roy, Rustum and Brindley, G. W. (1956) A study of the hydrothermal reconstitution of the kaolin minerals: in *Clays and Clay Minerals, Proc. 4th Natl. Conf., State College, Pennsylvania, 1955,* Ada Swineford, ed., *Natl. Acad. Sci. Natl. Res. Counc. Publ.* **456,** Washington, D.C., 125–132.

Roy, Rustum and Osborn, E. F. (1954) The system Al_2O_3-SiO_2-H_2O: *Amer. Mineral.* **39,** 853–885.

Saalfeld, H. (1955) The hydrothermal formation of clay minerals from metakaolin: *Ber. Deut. Keram. Ges.* **32,** 150–152.

Schachtschabel, P. (1930) Dehydration and rehydration of kaolin: *Chem. Erde* **4,** 375–419.

Siever, R. (1962) Silica solubility, 0°–200°C, and the diagenesis of siliceous sediments: *J. Geol.* **70,** 127–150.

Van Nieuwenberg, C. J. and Pieters, H. A. J. (1929) Rehydration of metakaolin and the synthesis of kaolin: *Ber. Deut. Keram. Ges.* **10,** 260–263.

Velde, B. and Kornprobst, J. (1969) Stabilité des silicates d'alumine hydrates: *Contrib. Mineral Petrol.* **21,** 63–74.

Walther, J. V. and Helgeson, H. C. (1977) Calculation of the thermodynamic properties of aqueous silica and the solubility of quartz and its polymorphs at high pressures and temperatures: *Amer. J. Sci.* **277,** 1315–1351.

Wefers, Karl and Bell, G. M. (1972) Oxides and hydroxides of aluminum: Technical Paper No. 19, Alcoa Research Laboratories, Pittsburgh, Pennsylvania, 51 pp.

(Received 18 April 1984; accepted 28 June 1984)

Резюме—На основе гидротермальных экспериментов были усовершенствованы три кривые давление-температура-время для системы Al_2O_3-SiO_2-H_2O и были определены реверсные температуры для двух из числа основных реакций, включающих каолинит. Величины температуры трех изобарных инвариантных точек позволили усовершенствовать величину свободной энергии Гиббса образования диаспора и пирофиллита, а также рассчитать поле стабильности каолинитов. Максимальная температура стабильного каолинита уменьшается от 296°C при давлении воды 2 кбар до 284°C при давлении жидкость/пар (для воды) и уменьшается быстро при низших давлениях. На изобарной кривой зависимости $[H_4SiO_4]$ от $°K^{-1}$, каолинит имеет клинообразное поле стабильности, которое расширяется по направлению к низшим температурам, чтобы включить большую часть $[H_4SiO_4]$ области близких к поверхности сред. Если $[H_4SiO_4]$ больше, чем для поля стабильности каолинита и температура <100°C, галлуазит образуется вместо пирофиллита, необычного педогенического материала. Пирофиллит легко образуется вместо каолинита при температуре свыше 150°C, если $[H_4SiO_4]$ контролируется кристобалитом или некристаллическим кремнеземом.

Каолинит и обычний предшественник, галлуазит, являются характерными продуктами выветривания и гидротермальных изменений пород. В осадочных отложениях сохранилось сравнительно небольшое количество галлуазита вследствие его низкой температуры дегидратации и нестабильности при низких давлениях воды, тогда как каолинит обычно сохраняется со времени девонского периода. В захороненных осадочных отложениях необходимые для стабильного каолинита давление воды и количество $[H_4SiO_4]$ в основном поддерживаются. В окисленных отложениях и в отложениях с уменьшенным количеством пирита каолинит обычно сохраняется, но каолинит стремится видоизмениться в иллит, цеолит, бертьерин или другие минералы там, где в жидкости пор сосредотачиваются щелочи, щелочные почвы или осадочное железо. [E.G.]

Resümee—Aus hydrothermalen Experimenten wurden drei Druck-Temperatur-Zeit-Kurven für das System Al_2O_3-SiO_2-H_2O bestimmt, und die Temperaturen für zwei der wichtigsten Kaolinitreaktionen gewonnen. Die Temperaturen von drei isobar invarianten Punkten ermöglichen die Bestimmung der Gibbs'schen Freien Energie für die Bildung von Diaspor und Pyrophyllit und die Berechnung des Stabilitätsfeldes von Kaolinit. Die maximale Temperatur für stabilen Kaolinit nimmt von 296°C bei 2 kBar Wasserdampfdruck auf 284°C bei gesättigtem Wasserdampfdruck ab und verringert sich sehr schnell bei niedrigeren Drucken. Auf einem isobaren Diagramm, in dem $[H_4SiO_4]$ gegen $°K^{-1}$ aufgetragen ist, hat Kaolinit ein keilförmiges Stabilitätsfeld, das sich gegen niedrigere Temperaturen hin verbreitert, um viel von $[H_4SiO_4]$-Bereich der Oberflächenzone mit einzuschließen. Wenn $[H_4SiO_4]$ über dem Kaolinitstabilitätsfeld liegt, und die Temperatur unter 100°C ist, dann bildet sich eher Halloysit als Pyrophyllit, ein unübliches Bodenmineral. Pyrophyllit bildet sich sehr leicht anstelle von Kaolinit bei Temperaturen über 150°C,wenn $[H_4SiO_4]$ durch Cristobalit oder nichtkristallisiertes SiO_2 kontrolliert wird.

Kaolinit und eine häufige Übergangsphase, Halloysit, sind typische Produkte der Verwitterung und hydrothermalen Umwandlung. In Sedimenten ist relativ wenig Halloysit aufgrund seiner niedrigen Dehydratationstemperatur und seiner Instabilität bei niedrigem H_2O-Druck zu finden, während Kaolinit im allgemeinen seit dem Devon überlebt hat. In Versenkungssedimenten bleiben der für stabilen Kaolinit geforderte H_2O-Druck und die notwendige $[H_4SiO_4]$-Aktivität im allgemeinen erhalten. In oxidierten Sedimenten und in pyritisch reduzierten Sedimenten bleibt Kaolinit gewöhnlich erhalten. Wenn jedoch Alkalien, Erdalkalien oder hydratisiertes Eisen in den Porenlösungen konzentriert sind, dann wandelt sich Kaolinit leicht in Illit, Zeolithe, Berthierit und anderen Minerale um. [U.W.]

Résumé—A partir d'expériences hydrothermiques, 3 courbes pression-température-temps ont été rafinées pour le système Al_2O_3-SiO_2-H_2O et des températures de revers ont été établies pour deux des réactions principales impliquant la kaolinite. Les températures de trois points invariants isobariques permet le rafinement de l'énergie libre de Gibbs de formation de la diaspore et de la pyrophyllite et le calcul du champ de stabilité de la kaolinite. La température maximale de kaolinite stable décroit de 296°C a 2 kb de pression d'eau a 284°C à la pression liquide/vapeur d'eau, et décroit rapidement à des pressions plus basses. Sur un diagramme isobarique de $[H_4SiO_4]$ vs. $°K^{-1}$, la kaolinite a un champ de stabilité éffilé à trois coins qui s'élargit vers la température plus basse pour inclure une grande partie de la gamme $[H_4SiO_4]$ d'environements proches de la surface. Si $[H_4SiO_4]$ est au delá du champ de stabilité de la kaolinite et la température est <100°C, l'halloysite est formée plutôt que la pyrophyllite, un minéral pédogénique peu commun. La pyrophyllite est formée promptement à la place de la kaolinite au delá de 150°C si $[H_4SiO_4]$ est contrôlée par la cristobalite ou par la silice non cristalline.

La kaolinite et un précurseur commun, l'halloysite, sont des produits caractéristiques de l'altération à l'air et hydrothermique. Dans des sédiments, relativement peu d'halloysite a survécu à cause de sa température de déshydratation basse et de son instabilité à de basses pressions d'eau, mais la kaolinite a communément survécu depuis la période dévonienne. Dans des sédiments ensevelis, la pression d'eau et l'$[H_4SiO_4]$ nécéssaires pour la kaolinite stable sont généralement maintenues. Dans des sédiments oxidés et dans des sédiments pyritiques réduits, la kaolinite a communément survécu, mais là où des alkalins, des terres alkalines, ou du fer aqueux a été concentré dans les fluides de pores, la kaolinite a eu tendance à se transformer en illite, zéolite, berthierine ou en d'autres minéraux. [D.J.]